[3] Diffraction of light beam on microstructured fiber

Sotsky A.B., Belskaya O.A.
Mogilev State A. Kuleshov University
Sotskaya L.I.
Belarusian-Russian University

Abstract

A method based on the Green's theorem and the Graph's addition theorem is used to construct a solution of 2D problem on lateral diffraction of a light beam on a microstructured fiber formed with a finite number system of parallel cylinders enclosed in a restricted shell. It is shown that the solution can be used for computing the angular distribution of the far field intensity in the case of three-dimensional beam diffraction on a microstructured fiber. Diffraction fields appeared at illumination of microstructured fibers by TE and TM polarized Gaussian beams are analyzed.

Introduction

It is known from experiments that intensity of the scattered light in lateral lighting of the microstructured fiber (MF) is sensitive to its internal structure [1-4]. This opens up a new opportunity for nondestructive diffraction control of microstructured fiber parameters by measuring the angular distribution of the designated intensity $S(\gamma)$. Such control is important in manufacturing micro-structured tapers intended for frequency filters and optical sensors [2-6]. Study of lateral light diffraction on the microstructured fiber is also of interest due to the development of sensory elements in optical object-deformation sensors [7, 8] and the upgraded diffractive element media filling up internal micropores of the microstructured fiber [1]. Similar calculations may be also used to estimate applicability limits of dielectric permittivity models of composite media [9].

Searching of quantitative correspondence between microstructured fiber parameters and the distribution $S(\gamma)$ supposes the solution of the corresponding diffraction problem. It is natural to use herein a model in which the microstructured fiber is represented by a set of a finite number of parallel cylinders enclosed in a shell with a restricted cross section [1-7].

Various methods of calculation of optical fields have been proposed so far scattered with parallel dielectric cylinder systems possessing (see [10, 12-14, 16, 17]) or, more generally, not possessing (see [11, 15, 18]) the circular symmetry. These methods can be applied in situations when the cylinders are surrounded by the infinite homogeneous medium [10, 11, 14, 15, 18], implemented in a semi-infinite substrate [17] or located within a plane-parallel layer of a finite thickness [13, 16]. However, in order to solve a diffraction problem on searching $S(\gamma)$ they are not applicable since they don't enable to consider the light reflection from an external contour boundary of the microstructured fiber.

This paper proposes the method of diffraction field calculation free of the specified limitation. It allows calculate the function $S(\gamma)$ being implemented in a far control area which is of interest for measuring in lateral lighting of the microstructured fiber with a limited light beam. The method represents a generalized approach developed in [18] when analyzing the eigenmodes of the microstructured fibers. Feasibility of the method is validated herewith below in section 2. Section 3 illustrates the internal convergence of the method and gives examples of computation of distributions $S(\gamma)$ being implemented in the microstructured fiber with different internal structures lighted with Gaussian light beams.

1. Method of calculation

Let us consider the dielectric microstructured fiber oriented along its uniformity axis $0z$. Its cross section is shown in Figure 1a. A curve line shows herein the fiber external boundary. It lies between circles with the radius $\rho = A$ and $\rho = B \geq A$. In the area $\rho > B$ lies the

homogenous medium with the relative dielectric permittivity ε_a. Inside of the fiber there are k cylinders of the composite (generally) section. The relative dielectric permittivity of the internal area of the j-cylinder is equal to ε_j and it may depend on the transverse coordinates. The cylinders are surrounded by a uniform sheath with its relative permittivity ε_s. The value ε_a is supposed to be a real quantity, and ε_j sand ε_s may be the complex values.

Assume that the microstructured fiber is lighted with a spatially limited monochromatic light beam with a time multiplier factor $\exp(i\omega t)$ (hereinafter omitted). The beam falls normally with respect to the axis $0z$. Under the plane of beam incidence we understand the plane $z = 0$. The beam axis makes an angle ψ with the coordinate axis $0y$. The intensity of the scattered field is recorded by a matrix of photoelectric receivers Φ located when $y' = L$ and lying in the far area ($k_0 L \gg 1$, where $k_0 = \omega\sqrt{\varepsilon_0\mu_0} = 2\pi / \lambda_0$ − is a vacuum wave number).

In the aforementioned description we have used a proper Cartesian coordinate system of the microstructured fiber $0xyz$, global polar coordinates ρ, φ, and local polar coordinates ρ_j, φ_j for each of the cylinders, as well as the Cartesian coordinate system of the incident beam $0x'y'z$, in which the axis $0y'$ coincides with the beam axis (Fig.1a).
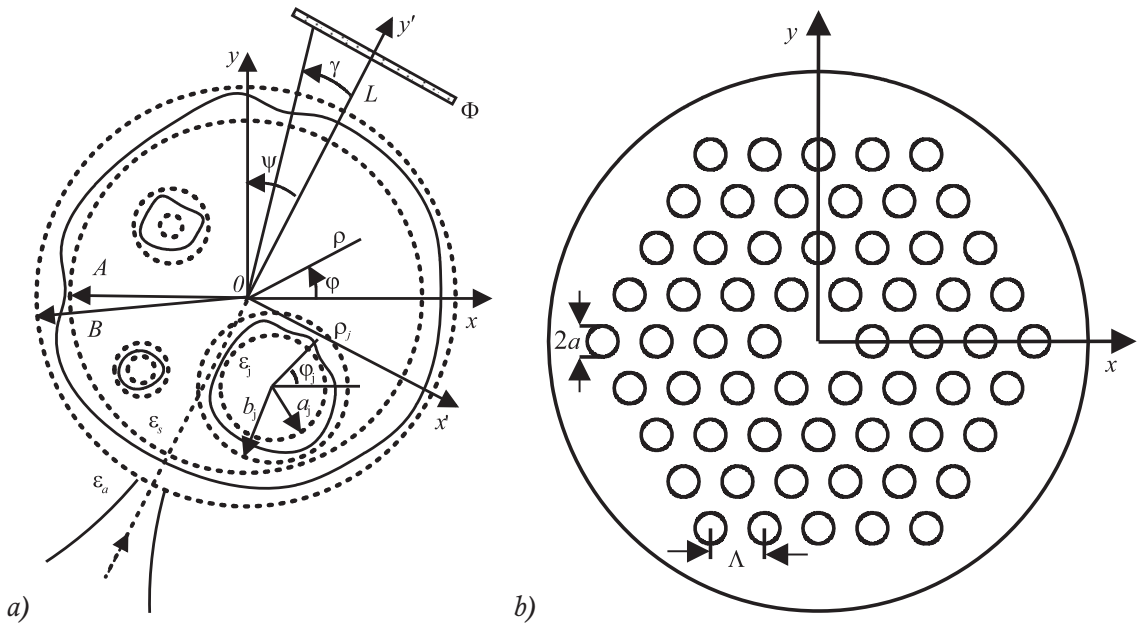

Fig.1. General view of the cross section of the considered microstructured fibers (a)
and the cross section of the microstructured fiber with the hexagonal symmetry (b)

We show that the calculation of the scattered field in the far area can be reduced to the solution of 2D diffraction problem.

Any Cartesian component F of the scattered optical field in the homogenous area $y' \geq B$ can be represented with the integral below [18]

$$F(x', y', z) = (y' - B)(2\pi)^{-1} \times$$
$$\times \int_{-\infty}^{\infty} dx_1 \int_{-\infty}^{\infty} dz_1 \frac{F(x_1, B, z_1)(1 + ik_a R)}{R^3 \exp(ik_a R)}, \quad (1)$$

when $k_a = k_0\sqrt{\varepsilon_a}$,

$$R = \sqrt{(x_1 - x')^2 + (z_1 - z')^2 + (y' - B)^2}.$$

Effective integration ranges according to the variables x_1 and z_1 in (1) have the radius order of the exciting beam w. Therefore in the far area, i.e. when

$$r = \sqrt{x'^2 + y'^2 + z^2} \gg w, \ y' \gg B,$$

$k r \gg$ the equation (1), by means of the expansion R in powers of x_1 / r, z_1 / r, B / r, can be reduced to the following form

$$F(x', y', z) = \frac{ik_a y'}{2\pi r^2} \exp\left(-ik_a r + ik_a B \frac{y'}{r}\right) \times$$
$$\times \int_{-\infty}^{\infty} dx_1 \int_{-\infty}^{\infty} F(x_1, B, z_1) \exp\left[\frac{ik_a}{r}(x_1 x' + z_1 z)\right] dz_1 \times \quad (2)$$
$$\times [1 + O(k_0 r)^{-1}].$$

Hereinafter we will have interest in the distribution of the far scattered field in the plane of beam incidence. In this case Eq. (2) can be simplified as follows:

$$F(x', y', 0) = \frac{ik_a \cos\gamma}{\rho} \exp[ik_a(B\cos\gamma - \rho)] \times$$
$$\times \int_{-\infty}^{\infty} \frac{\hat{F}(x_1, B, 0)}{\exp(ik_a x_1 \sin\gamma)} dx_1 \cdot [1 + O(k_0\rho)^{-1}], \quad (3)$$

where $\rho = \sqrt{x'^2 + y'^2}$, γ – is the angle at a viewpoint (Fig.1a),

$$\hat{F}(x_1, B, 0) = (2\pi)^{-1} \int_{-\infty}^{\infty} F(x_1, B, z_1) dz_1 \quad (4)$$

In order to set $\hat{F}(x_1, B, 0)$, let us assume the electromagnetic field by Fourier integrals at z:

$$\mathbf{E}(x', y', z) = \int_{-\infty}^{\infty} \exp(-i\beta z)\hat{\mathbf{E}}(x', y', \beta) d\beta \quad (5)$$

$$\mathbf{H}(x', y', z) = \int_{-\infty}^{\infty} \exp(-i\beta z)\hat{\mathbf{H}}(x', y', \beta) d\beta \quad (6)$$

Substituting Eq. (5) and (6) to Maxwell's equations shall result to differential equations with respect to vectors' components

$$\hat{\mathbf{E}}(x', y', \beta) = \frac{1}{2\pi} \int_{-\infty}^{\infty} \exp(i\beta z)\mathbf{E}(x', y', z) dz \quad (7)$$

$$\hat{\mathbf{H}}(x', y', \beta) = \frac{1}{2\pi} \int_{-\infty}^{\infty} \exp(i\beta z)\mathbf{H}(x', y', z) dz \quad (8)$$

Since the microstructured fiber parameters do not depend on z, these equations related to different β are considered to be independent. They formally coincide with equations (1.4.10) – (1.4.15) given in monograph [20] which describe mode fields of optical waveguides. When $\beta = 0$, these equations shall correspond to 2D diffraction problem in which $\partial/\partial z \equiv 0$, and instead of $\mathbf{E}(x', y', z)$ and $\mathbf{H}(x', y', z)$, occur $\hat{\mathbf{E}}(x', y', 0)$ and $\hat{\mathbf{H}}(x', y', 0)$, respectively. It follows therefrom that functions $\hat{F}(x_1, B, 0)$ in form of (4) may be calculated as a result of solution of the given 2D problem in which excitation of the microstructured fiber is carried out by the two-dimensional beam with the field $\hat{\mathbf{E}}(x', y', 0)$, $\hat{\mathbf{H}}(x', y', 0)$, connected with the field of the actual three-dimensional beam $\mathbf{E}(x', y', z)$, $\mathbf{H}(x', y', z)$ by Fourier transforms (7) and (8).

A two-dimensional analogue of (1) is [19]

$$\hat{F}(x', y', 0) = \frac{y' - B}{\pi} \int_{-\infty}^{\infty} dx_1 \hat{F}(x', B, 0) \times$$
$$\times \frac{\exp(-ik_a R)}{R^2} \int_{-\infty}^{\infty} \frac{\exp(-\tau^2)(\tau^2 + ik_a R)}{\sqrt{\tau^2 + 2ik_a R}} d\tau, \quad (9)$$

where R is calculated for $z_1 = 0$. Provided $\rho \gg w$, $y' \gg B$, $k_0\rho \gg 1$ (9) shall be reduced to the following form:

$$\hat{F}(x', y', 0) = \sqrt{\frac{ik_a}{2\pi\rho}} \cos\gamma \exp[ik_a(B\cos\gamma - \rho)] \times$$
$$\times \int_{-\infty}^{\infty} \frac{\hat{u}(_1, , 0)}{\exp(\hat{u}_a {}_1 \sin\gamma)} dx_1 \cdot [1 + O(k_0\rho)^{-1}]. \quad (10)$$

If compare Eq. (3) and (10), we can come to the conclusion that within small limits $O(k_0\rho)^{-1}$

$$F(x', y', 0) = \sqrt{2\pi i k_a \rho^{-1}}\ \hat{F}(x', y', 0) \quad (11)$$

From Eq. (11) it follows that in order to find the distribution of the far scattered field in the plane of incidence on the microstructured fiber of the three-dimensional beam, it would be sufficient to calculate the similar field in the described 2D problem.

In 2D problem it would be possible to separately consider TM ($\hat{E}_z \equiv 0$, $\hat{H}_x \equiv 0$, $\hat{H}_y \equiv 0$) and TE ($\hat{H}_z \equiv 0$, $\hat{E}_x \equiv 0$, $\hat{E}_y \equiv 0$) polarized waves [20].

Thus, TM polarized waves shall be governed by the following equation:

$$\left(\frac{\partial}{\partial x} \frac{1}{\varepsilon} \frac{\partial}{\partial x} + \frac{\partial}{\partial y} \frac{1}{\varepsilon} \frac{\partial}{\partial y} + k_0^2 \right) \hat{H}_z = 0 \quad (12)$$

Applying the Green's theorem to Eq. (12) according to the scheme described in [19], it is possible to obtain the following integral equation:

$$\sum_{j=1}^{k} \Omega_j(x, y) + \Omega(x, y) = W(x, y) \quad (13)$$

Here
$$\Omega_j(x, y) = b_j \int_0^{2\pi} \left[G(r) \frac{\partial \hat{H}_z(x', y', 0)}{\partial \rho'_j} - \right.$$
$$\left. - \hat{H}_z(x', y', 0) \frac{\partial G(r)}{\partial \rho'_j} \right] d\varphi'_j, \quad (14)$$

$$\Omega(x, y) = -A \int_0^{2\pi} \left[G(r) \frac{\partial \hat{H}_z(x', y', 0)}{\partial \rho'} - \right.$$
$$\left. - \hat{H}_z(x', y', 0) \frac{\partial G(r)}{\partial \rho'_j} \right] d\varphi', \quad (15)$$

$$G(r) = \frac{iH_0^{(2)}(k_s r)}{4}, \quad k_s = k_0\sqrt{\varepsilon_s}, \quad r = \sqrt{(x' - x)^2 + (y' - y)^2},$$

$H_0^{(2)}(k_s r)$ – is the Hankel function, $W(x, y) \equiv 0$, provided $\rho > A$, and $\rho_j < b_j$, $W(x, y) \equiv \hat{H}_z(x, y, 0)$ in the remaining space. The shaded coordinates in (14) and (15) are determined according to the formulas $x' = x_j + b_j \cos\varphi'_j$, $y' = y_j + b_j \sin\varphi'_j$ and $x' = A\cos\varphi'$, $y' = A\sin\varphi'$, where x_j, y_j – are the coordinates of the center of the j – cylinder.

In order to algebraize the equation (13) let us assume the field within the areas $\rho_j \leq b_j$ ($j = 1, k$) and $\rho \geq A$ by Fourier polynomials:

$$\left. \begin{array}{l} \hat{H}_z = \sum_{\nu=-m}^{m} h_\nu^{(j)}(\rho_j) \exp(i\nu\varphi_j), \\[2mm] -i\omega\varepsilon_0 \hat{E}_{\varphi_j} = \varepsilon^{-1}\partial\hat{H}_z / \partial\rho_j = \sum_{\nu=-m}^{m} e_\nu^{(j)}(\rho_j) \exp(i\nu\varphi_j), \end{array} \right\} \quad (16)$$

$$\hat{H}_z = \sum_{v=-n}^{n} h_v(\rho)\exp(iv\varphi),$$
$$-i\omega\varepsilon_0\hat{E}_\varphi = \varepsilon^{-1}\partial\hat{H}_z / \partial\rho = \sum_{v=-n}^{n} e_v(\rho)\exp(iv\varphi),$$
(17)

where m and n – are the reduction orders of Fourier's series by the angular variables φ_j and φ. After substituting (16) and (17) to (12) and after using orthogonality relations for exponents we come to ordinary differential equations:

$$\frac{dh_v^{(j)}}{d\rho_j} = \sum_{\mu=-m}^{m} \varepsilon_{jv\mu} e_\mu^{(j)},$$
$$\frac{de_v^{(j)}}{d\rho_j} = -k_0^2 h_v^{(j)} - \frac{e_v^{(j)}}{\rho_j} + \frac{v}{\rho_j^2}\sum_{\mu=-m}^{m} \mu\,\varepsilon_{jv\mu}^{-1} h_\mu^{(j)},$$
(18)

$$\frac{dh_v}{d\rho} = \sum_{\mu=-n}^{n} \varepsilon_{v\mu} e_\mu,$$
$$\frac{de_v}{d\rho} = -k_0^2 h_v - \frac{e_v}{\rho} + \frac{v}{\rho^2}\sum_{\mu=-m}^{m} \mu\,\varepsilon_{v\mu}^{-1} h_\mu,$$
(19)

where
$$\varepsilon_{jv\mu} = \frac{1}{2\pi}\int_0^{2\pi} \exp[i(\mu-v)\varphi_j]\varepsilon(\rho_j,\varphi_j)d\varphi_j,$$
$$\varepsilon_{jv\mu}^{-1} = \frac{1}{2\pi}\int_0^{2\pi} \exp[i(\mu-v)\varphi_j]\varepsilon^{-1}(\rho_j,\varphi_j)d\varphi_j,$$
(20)

$$\varepsilon_{v\mu} = \frac{1}{2\pi}\int_0^{2\pi} \exp[i(\mu-v)\varphi]\varepsilon(\rho,\varphi)d\varphi,$$
$$\varepsilon_{v\mu}^{-1} = \frac{1}{2\pi}\int_0^{2\pi} \exp[i(\mu-v)\varphi]\varepsilon^{-1}(\rho,\varphi)d\varphi.$$
(21)

Let us assume that in the j-cylinder round the origin of coordinates a certain circle with the radius a_j can be described, within the limits of which the dielectric permittivity is constant (Fig.1a). According to Eq. (18), in this circle $\varepsilon_{jv\mu} = \delta_{v\mu}\varepsilon_j$, $\varepsilon_{jv\mu}^{-1} = \delta_{v\mu}\varepsilon_j^{-1}$, where $\delta_{v\mu}$ – is the Kronecker symbol. Then the system (18) is reduced to independent Bessel's equations. Solutions of these equations are physically meaningful being regular when $\rho_j \to 0$. Therefore within the range of $\rho_j \le a_j$ it should be set as follows:

$$h_v^{(j)}(\rho_j) = C_v^{(j)} J_v(k_j\rho_j),$$
$$e_v^{(j)}(\rho_j) = \frac{k_0^2 C_v^{(j)}}{2k_j}\left[J_{v-1}(k_j\rho_j) - J_{v+1}(k_j\rho_j) \right],$$
(22)

where $k_j = k_0\sqrt{\varepsilon_j}$, $J_v(...)$ – is the Bessel's function, $C_v^{(j)}$ – are certain coefficients. Then the general solution of the system (18) can be equated as follows:

$$h_v^{(j)}(\rho_j) = \sum_{\mu=-}^{} P_{v\mu}^{(j)}(\rho_j) C_\mu^{(j)},$$
$$e_v^{(j)}(\rho_j) = \sum_{\mu=-}^{} Q_{v\mu}^{(j)}(\rho_j) C_\mu^{(j)},$$
(23)

where $P_{v\mu}^{(j)}(\rho_j) = h_v^{(j)}(\rho_j)$, $Q_{v\mu}^{(j)}(\rho_j) = e_v^{(j)}(\rho_j)$ and it is understood that right-hand sides of the last two equations are calculated as the result of solving simultaneous equations (18) on the interval $[a_j, \rho_j]$ with starting conditions

$$h_v^{(j)}(a_j) = \delta_{v\mu} J_\mu(k_j a_j)$$
(24)

$$e_v^{(j)}(a_j) = \frac{\delta_{v\mu} k_0^2}{2k_j}\left[J_{\mu-1}(k_j a_j) - J_{\mu+1}(k_j a_j) \right].$$
(25)

Supposing in (14) [21] that
$$H_0^{(2)}(k_s r) = \sum_{v=-\infty}^{\infty} \exp\left[iv(\varphi_j - \varphi_j')\right]\times$$
$$\times\begin{cases} H_v^{(2)}(k_s\rho_j')J_v(k_s\rho_j) & \text{at } \rho_j < \rho_j' \\ J_v(k_s\rho_j')H_v^{(2)}(k_s\rho_j) & \text{at } \rho_j > \rho_j' \end{cases},$$
we can reduce this equation to
$$\Omega_j(x,y) = \sum_{v=-m}^{m} Z_v^{(l)}(\rho_j,\varphi_j) \sum_{\mu=-m}^{m} U_{jv\mu}^{(l)} C_\mu^{(j)}$$
(26)

when $l = 1$ provided $\rho_j < b_j$, and $l = 2$ provided $\rho_j \ge b_j$,
$$U_{jv\mu}^{(l)} = 0,5i\pi k_s b_j\left[k_0^{-1}\sqrt{\varepsilon_s}\,\bar{Z}_{jv}^{(l)} Q_{v\mu}^{(j)}(b_j) - \right.$$
$$\left. -0.5(\bar{Z}_{jv-1}^{(l)} - \bar{Z}_{jv+1}^{(l)})P_{v\mu}^{(j)}(b_j) \right],$$
(27)
$$Z_v^{(l)}(\rho,\varphi) = \exp(iv\varphi)[(2-l)J_v(k_s\rho) + (l-1)H_v^{(2)}(k_s\rho)],$$
$$\bar{Z}_{jv}^{(l)} = (2-l)H_v^{(2)}(k_s b_j) + (l-1)J_v(k_s b_j).$$

In order to convert the function $\Omega(x,y)$, we shall consider that the field outside the fiber (area $\rho \ge B$) can be represented as follows [22]

$$\hat{H}_z = \sum_{v=-n}^{n} D_v^{(1)} J_v(k_a\rho)\exp(iv\varphi) +$$
$$+ \sum_{v=-n}^{n} D_v^{(2)} H_v^{(2)}(k_a\rho)\exp(iv\varphi),$$
(28)

when $k_a = k_0\sqrt{\varepsilon_a}$. The first sum in (28), where
$$D_v^{(1)} = \frac{\int_0^{2\pi} \hat{H}_z^{(i)}(B\cos\varphi, B\sin\varphi, 0)\exp(-iv\varphi)d\varphi}{2\pi J_v(k_a B)}$$
(29)

describes the incident beam with the magnetic component $H_z^{(i)}(x,y,z)$, and the second sum describes the field scattered by the microstructured fiber, where the coefficients $D_v^{(2)}$ are to be determined.

Repeating the calculations similar to the above mentioned, we determine the following:
$$\Omega(x,y) = \sum_{v=-n}^{n} Z_v^{(l)}(\rho,\varphi)\sum_{p=1}^{2}\sum_{\mu=-n}^{n} V_{v\mu}^{(lp)} D_\mu^{(p)}$$
(30)

when $l = 1$ provided $\rho < A$, and $l = 2$ provided $\rho \ge A$,
$$V_{v\mu}^{(lp)} = -0,5i\pi k_s A\left[k_0^{-1}\sqrt{\varepsilon_s}\,\bar{Z}_v^{(l)} T_{v\mu}^{(p)}(A) - \right.$$
$$\left. -0.5(\bar{Z}_{v-1}^{(l)} - \bar{Z}_{v+1}^{(l)})R_{v\mu}^{(p)}(A) \right],$$
$$\bar{Z}_v^{(l)} = (2-l)H_v^{(2)}(k_s A) + (l-1)J_v(k_s A),$$
(31)

$R_{\nu\mu}^{(p)}(\rho) = h_\nu(\rho)$, $T_{\nu\mu}^{(p)}(\rho) = e_\nu(\rho)$; $h_\nu(\rho)$ and $e_\nu(\rho)$ are calculated as the result of solving simultaneous equations (19) on the interval $[\rho, B]$ under starting conditions

$$h_\nu(B) = \delta_{\nu\mu}\left[(2-p)J_\mu(k_a B) + (p-1)H_\mu^{(2)}(k_a B)\right] \quad (32)$$

$$e_\nu(B) = \frac{\delta_{\nu\mu}k_0^2}{2k_a}\left\{(2-p)\left[J_{\mu-1}(k_a B) - J_{\mu+1}(k_a B)\right] + \right.$$
$$\left. +(p-1)\left[H_{\mu-1}^{(2)}(k_a B) - H_{\mu+1}^{(2)}(k_a B)\right]\right\}. \quad (33)$$

The equations (26) and (30) are written using the local polar coordinates for all cylinders and the global polar coordinates. However the Graph's addition theorem [21] allows us to reduce each of these equations to any of the indicated coordinate systems. As the result of this, in the area $\rho > A$, as well as in all cylinders areas, the equation (13) shall be reduced to the form

$$\sum_{\nu=-n}^{n} Z_\nu^{(2)}(\rho, \varphi)\Phi_\nu = 0 \quad (34)$$

$$\sum_{\nu=-m}^{m} Z_\nu^{(1)}(\rho_j, \varphi_j)\Psi_{j\nu} = 0 \quad (35)$$

$$\Phi_\nu = \sum_{j=1}^{k}\sum_{\mu=-m}^{m} Z_{\nu-\mu}^{(1)}(\rho^{(j)}, \varphi^{(j)})\sum_{\sigma=-m}^{m} U_{j\mu\sigma}^{(2)}C_\sigma^{(j)} + $$
$$+\sum_{p=1}^{2}\sum_{\mu=-n}^{n} V_{\nu\mu}^{(2p)}D_\mu^{(p)}, \quad (36)$$

$$\Psi_{j\nu} = \sum_{\mu=-m}^{m} U_{j\nu\mu}^{(1)}C_\mu^{(j)} + $$
$$+\sum_{l\neq j}\sum_{\mu=-m}^{m} Z_{\mu-\nu}^{(2)}(\rho^{(lj)}, \varphi^{(lj)})\sum_{\sigma=-m}^{m} U_{l\mu\sigma}^{(2)}C_\sigma^{(l)} + \quad (37)$$
$$+\sum_{\mu=-n}^{n} Z_{\mu-\nu}^{(1)}(\rho^{(j)}, \varphi^{(j)})\sum_{\sigma=-n}^{n}\sum_{p=1}^{2} V_{\mu\sigma}^{(1p)}D_\sigma^{(p)},$$

$\rho^{(j)}$, $\varphi^{(j)}$ – are the global polar coordinates of origin of the local coordinate system of the j-cylinder, $\rho^{(lj)}$, $\varphi^{(lj)}$ – are the polar coordinates of origin of the local coordinate system of the j-cylinder in the coordinate system of the l-cylinder.

The functions $Z_\nu^{(2)}(\rho, \varphi)$ in (34) and $Z_\nu^{(1)}(\rho_j, \varphi_j)$ in (35), related to different ν, are linearly independent, therefore (34) and (35) are equivalent to the system of algebraic equations

$\Phi_\nu = 0$ $(\nu = \overline{-n, n})$, $\Psi_{j\nu} = 0$ $(j = \overline{1, k}, \nu = \overline{-m, m})$ with respect to the coefficients $C_\mu^{(j)}$ and $D_\nu^{(2)}$. In accordance with (36), (37) this system takes the following form:

$$\sum_{\beta=1}^{N} M_{\alpha\beta}X_\beta = \sum_{\kappa=-n}^{n} K_{\alpha\kappa}D_\kappa^{(1)} \quad (38)$$

Here, provided $1 \leq \alpha \leq k(2m+1)$

$$X_\alpha = C_\nu^{(j)}, \quad K_{\alpha\kappa} = -\sum_{\sigma=-n}^{n} Z_{\sigma-\nu}^{(1)}(\rho^{(j)}, \varphi^{(j)})V_{\sigma\kappa}^{(11)},$$

$$M_{\alpha\beta} = H[k(2m+1)-\beta]\times$$
$$\times\left[\delta_{jl}U_{j\nu\mu}^{(1)} + (1-\delta_{jl})\sum_{\sigma=-m}^{m} Z_{\sigma-\nu}^{(2)}(\rho^{(lj)}, \varphi^{(lj)})U_{l\sigma\mu}^{(2)}\right] + $$
$$+H[\beta - k(2m+1)-1]\sum_{\sigma=-n}^{n} Z_{\sigma-\nu}^{(1)}(\rho^{(j)}, \varphi^{(j)})V_{\sigma\mu}^{(12)},$$

whereas $k(2m+1) < \alpha \leq N$
$$X_\alpha = D_\nu^{(2)}, \quad K_{\alpha\kappa} = -V_{\nu\kappa}^{(21)},$$
$$M_{\alpha\beta} = H[k(2m+1)-\beta]\sum_{\sigma=-m}^{m} Z_{\nu-\sigma}^{(1)}(\rho^{(l)}, \varphi^{(l)})U_{l\sigma\mu}^{(2)} + $$
$$+H[\beta - k(2m+1)-1]V_{\nu\mu}^{(22)};$$
$$= \zeta(\alpha), \quad l = \zeta(\beta), \quad \nu = \tau(\alpha), \quad \mu = \tau(\beta),$$
$$\tau(x) = H[k(2m+1)-x][x+m-\zeta(x)(2m+1)] + $$
$$+H[x-k(2m+1)-1][x-k(2m+1)-n-1],$$
$$H(x) = 1 \text{ at } x \geq 0, \quad H(x) = 0 \text{ at } x < 0,$$
$$\zeta(x) = \text{int}[(x-1)(2m+1)^{-1}] + 1,$$
$\text{int}[\ldots]$ means a truncation.

In accordance with (28) and (38), calculation of the two-dimensional field scattered by the microstructured fiber is reduced to calculation of the coefficients $D_\nu^{(2)}$ by the following formulas:

$$D_\nu^{(2)} = \sum_{\mu=-n}^{n} S_{\nu\mu}D_\mu^{(1)} \quad (39)$$

$$S_{\nu\mu} = \sum_{\alpha=1}^{N}\left(M^{-1}\right)_{\beta\alpha}K_{\alpha\mu} \quad (40)$$

where M^{-1} – is a matrix inverse to the matrix M of the equation (38), $\beta = k(2m+1) + \nu + n + 1$.

When calculating the far diffractive field, we can use in (28) the asymptotic representation of Hankel functions [21]

$$H_\nu^{(2)}(k_a\rho) = \sqrt{2(\pi k_a\rho)^{-1}}\exp\left[-i\left(k_a\rho - \frac{\nu\pi}{2} - \frac{\pi}{4}\right)\right]\times$$
$$\times[1 + O(k_0\rho)^{-1}],$$

whereas the far field of the incident beam may be described with the equation (10), when $B = 0$, $\tilde{F} = \hat{H}_z^{(i)}$. Thus, omitting small $O(k_0\rho)^{-1}$ and considering that $\varphi = 0,5\pi + \gamma - \psi$, in the area of $y' > 0$ (Fig.1a), we obtain the following:

$$\hat{H}_z(x', y', 0) = \sqrt{2i(\pi k_a\rho)^{-1}}\exp(-ik_a\rho)f(\gamma) \quad (41)$$

$$f(\gamma) = \frac{k_a\cos\gamma}{2}\int_{-\infty}^{\infty}\frac{\hat{H}_z^{(i)}(x_1, 0, 0)}{\exp(ik_a x_1\sin\gamma)}dx_1 + $$
$$+\sum_{\nu=-n}^{n} D_\nu^{(2)}\exp[i\nu(\pi + \gamma - \psi)], \quad (42)$$

where the field $H_z^{(i)}$ is set in the coordinate system $0x'y'z$.

In the considered 2D problem we can formally determine the far field intensity S_ρ in the semi-space $y' > 0$, beam powers per unit length $P_s^{(+)}$ and $P_s^{(-)}$ for

the emission scattered into semi-spaces $y' > 0$ and $y' < 0$, respectively, and the power per unit length for the incident beam P_i using the following formulas

$$S_\rho = k_0 Z (2k_a)^{-1} \left| \hat{H}_z \right|^2 \tag{43}$$

$$P_s^{(+)} = \rho \int_{-0,5\pi}^{0,5\pi} S_\rho \, d\gamma \tag{44}$$

$$P_s^{(-)} = \frac{k_0 Z}{\pi k_a^2} \int_{0,5\pi}^{1,5\pi} \left| \sum_{\nu=-n}^{n} D_\nu^{(2)} \exp[i\nu(\pi + \gamma - \psi)] \right|^2 d\gamma \tag{45}$$

$$P_i = \frac{k_0 Z}{4\pi k_a} \int_{-0,5\pi}^{0,5\pi} \left| \int_{-\infty}^{\infty} \frac{\hat{H}_z^{(i)}(x',0,0) \cos\gamma}{\exp(ik_a x' \sin\gamma)} dx' \right|^2 d\gamma, \tag{46}$$

when $Z = \sqrt{\mu_0 / \varepsilon_0}$. In case when the microstructured fiber consists of the media with real-valued dielectric permittivities, the equations (43) – (46) enable to control correctness of the solution (39) through testing the execution of the energy conservation law $(P_s^{(+)} + P_s^{(-)}) / P_i = 1$ (see Section 2).

If microstructured fibers are excited by TM polarized Gaussian beams, then for the scattered light intensity registered by the matrix of photoelectric receivers Φ in the plane $z = 0$ from (11), when $F = H_z$, $\hat{F} = \hat{H}_z$, (41) and (43) we determine:

$$S(\gamma) = \frac{2\pi k_a \cos\gamma}{\rho} S_\rho = \frac{2k_0 Z}{L^2 k_a} \cos^3\gamma \left| f(\gamma) \right|^2 \tag{47}$$

In practically important case of the microstructured fiber excited with the focused Gaussian beam we have:

$$H_z^{(i)}(x',y',z) = C w^2 (4\pi)^{-1} \times$$
$$\times \int_{-\infty}^{\infty} dk_1 \int_{-\infty}^{\infty} \exp[-i(\lambda y' + k_1 x' + k_2 z')] \times \tag{48}$$
$$\times \exp[-0,25(k_1^2 + k_2^2)w^2] dk_2,$$

when $\lambda = \sqrt{k_a^2 - k_1^2 - k_2^2}$, C – is an amplitude factor. Then under the actual experimental condition $\exp(-0,25k_a^2 w^2) \ll 1$ from (29), (42), (46), (48) we obtain:

$$D_\nu^{(1)} = C k_a w^2 (2\pi)^{-1} \exp[i\nu(\psi - \pi)] \times$$
$$\times \int_0^{0,5\pi} \frac{\cos(\gamma) \cos(\nu\gamma)}{\exp(0,25 k_a^2 w^2 \sin^2\gamma)} d\gamma, \tag{49}$$

$$f(\gamma) = C \frac{k_a w^2 \cos\gamma}{4 \exp(0,25 k_a^2 w^2 \sin^2\gamma)} +$$
$$+ \sum_{\nu=-n}^{n} D_\nu^{(2)} \exp[i\nu(\pi + \gamma - \psi)], \tag{50}$$

$$P_i = |C|^2 \frac{k_0 Z w^4}{8\pi} \int_0^{0,5\pi} \frac{\cos^2\gamma}{\exp(0,5 k_a^2 w^2 \sin^2\gamma)} d\gamma \tag{51}$$

The case with TE polarized waves (the electric-field vector is directed along the axis $0z$) may also be ana-

lyzed according to the above scheme. These waves are described by the following equation:

$$\left(\frac{\partial^2}{\partial x^2} + \frac{\partial^2}{\partial y^2} + k_0^2 \varepsilon \right) \hat{E}_z = 0,$$

therefore the analogues of decompositions (16) – (19) are as follows:

$$\left. \begin{aligned} \hat{E}_z &= \sum_{\nu=-m}^{m} h_\nu^{(j)}(\rho_j) \exp(i\nu\varphi_j), \\ i\omega\mu_0 \hat{H}_{\varphi_j} &= \partial \hat{E}_z / \partial \rho_j = \sum_{\nu=-m}^{m} e_\nu^{(j)}(\rho_j) \exp(i\nu\varphi_j), \end{aligned} \right\} \tag{52}$$

$$\left. \begin{aligned} \hat{E}_z &= \sum_{\nu=-n}^{n} h_\nu(\rho) \exp(i\nu\varphi), \\ i\omega\mu_0 \hat{H}_\varphi &= \partial \hat{E}_z / \partial \rho = \sum_{\nu=-n}^{n} e_\nu(\rho) \exp(i\nu\varphi), \end{aligned} \right\} \tag{53}$$

$$\left. \begin{aligned} \frac{dh_\nu^{(j)}}{d\rho_j} &= e_\nu^{(j)}, \\ \frac{de_\nu^{(j)}}{d\rho_j} &= -k_0^2 \sum_{\mu=-m}^{m} \varepsilon_{j\nu\mu} h_\mu^{(j)} - \frac{e_\nu^{(j)}}{\rho_j} + \left(\frac{\nu}{\rho_j} \right)^2 h_\nu^{(j)}, \end{aligned} \right\} \tag{54}$$

$$\left. \begin{aligned} \frac{dh_\nu}{d\rho} &= e_\nu, \\ \frac{de_\nu}{d\rho} &= -k_0^2 \sum_{\mu=-n}^{n} \varepsilon_{\nu\mu} h_\mu - \frac{e_\nu}{\rho} + \left(\frac{\nu}{\rho} \right)^2 h_\nu. \end{aligned} \right\} \tag{55}$$

The above remaining formulas obtained when analyzing TM polarized waves remain practically unchanged. Among them some upgrades are only required for formulas (28), (41) and (43), in which we must substitute $\hat{H}_z \to \hat{E}_z$, the formulas (29), (42), (46) and (48), in which $\hat{H}_z^{(i)} \to \hat{E}_z^{(i)}$ to be substituted, the formulas (22) and (25), in which $0.5 k_0^2 / k_j \to 0.5 k_j$ to be substituted, the formula (33), in which $k_0^2 / k_a \to k_a$ to be substituted and the formulas (27), (31), when $\sqrt{\varepsilon_s} \to 1$. Besides, in (43) (45), (46), (47), (51) we have to change Z / k_a to k_a / Z.

The solution of Eq. (39), (40) has been determined when considering the microstructured fiber whose internal cylinders and external boundaries have a complex cross-section (Fig. 1). In general, the calculation of matrix elements and absolute terms of the algebraic system (38) may be performed by numerical integration of the Cauchy problem (18) (or (54)), (24), (25) and (19) (or (55)), (32), (33) and may encounter no crucial difficulties [19]. Calculations may be considerably simplified if the aforesaid cylinders and boundaries possess the circular symmetry. In this case, the solution of these problems can be analytically expressed through cylindrical functions. For example, if the cylinders have the circular cross-section and ε_j does not depend on ρ_j, we can set $a_j = b_j$ ($j = 1,k$), $A = B$. Then $P_{\nu\mu}^{(j)}(b_j)$ and $Q_{\nu\mu}^{(j)}(b_j)$

in (27) will be equal to the right-hand sides of the equations (24) and (25), whereas $R_{\nu\mu}^{(p)}(A)$ and $T_{\nu\mu}^{(p)}(A)$ in (31) will be equal to the right-hand sides of the equations (32) and (33). The further reduction of the solution occurs if the ports inside of the fiber are missing ($b_j \to 0$, or $\varepsilon_j \to \varepsilon_s$ for all j). In this case a scattering matrix $S_{\nu\mu}$ becomes diagonal and the solution (39) coincides with the known analytical solution of the electromagnetic wave diffraction problem on a homogeneous circular cylinder [22].

2. Numerical examples

The accuracy of the solution (28), (39), (43)-(45), (47) is determined only by reduction orders of the Fourier series m and n. Its intrinsic convergence may be illustrated as described below by diffraction calculation results of TE and TM polarized Gaussian beams on the microstructured fibers with the hexagonal symmetry (1b). We have considered silica microstructured fibers with the circular external boundary surrounded with air and having the inner cylinders of the circular cross section filled with air. We have used a geometrical model of the microstructured fiber empirically identified in [6]. On condition that

$$A \le A_s = \left[a_0 (\beta A_0)^{-1} \right]^{\alpha^{-1}} (\bar{A} - A_c) + A_c$$

the following correlations are to be fulfilled therein $\Lambda = \Lambda_0 A A_0^{-1}$, $a_j = a$ $(j = 1, k)$,

$$a = \beta A \left[(A - A_c)(\bar{A} - A_c)^{-1} \right]^{\alpha} H(A - A_c),$$

$$A_c = \bar{A}[(0,51)^{\alpha^{-1}} - 0,78][(0,51)^{\alpha^{-1}} - 1]^{-1},$$

where Λ – is a distance between centers of adjoining cylinders (Fig.1b), Λ_0, a_0, A_0 $\bar{A}$, α, β – are the process invariables. Notice that provided $A \le A_c$, there occur blow-ups of the air ports within the microstructured fiber [6]. Calculations have been performed for different A and $\Lambda_0 = 5,5$ μm, $a_0 = 1,4$ μm, $A_0 = 62,5$ μm, $\bar{A} = 25$ μm, $\alpha = 0,35$, $\beta = 0,012$, $A_s = 56,88$ μm, $A_c = 18,56$ μm, $w = 5$ μm, $\lambda_0 = 0,6328$ μm, $\varepsilon_a = \varepsilon_j = 1$ $(j = 1, k)$, $\varepsilon_s = 2,093243$ [6]. We have studied the microstructured fiber in which the fiber geometric center, with no air gate available, is surrounded by four hexagonal rings of the air ports (Fig. 1b). The angle ψ, which characterizes the orientation of the beam axis in respect to the coordinate system of the microstructured fiber (Fig.1a), has been selected equal to 0.

The table and Figure 2 below illustrate the intrinsic convergence of the method. They correspond to excitation of the microstructured fiber with $A = 35$ μm ($\Lambda = 3,080$ μm, $a = 0,583$ μm) by TE polarized Gaussian beams.

Table. Power balance in particular reduction orders of the Fourier's series m and n

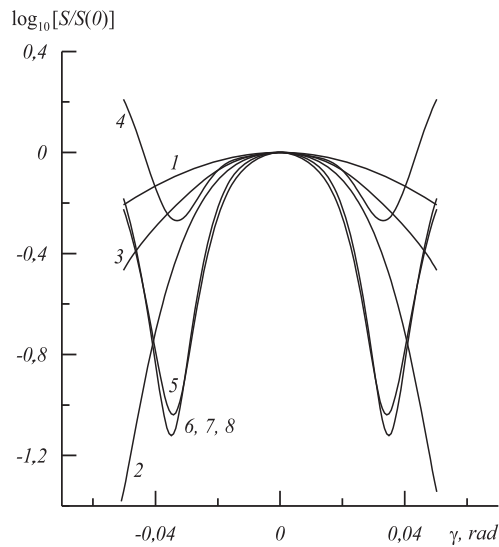| №	m	n	$(P_s^{(+)} + P_s^{(-)}) / P_i$
1	0	100	0.95359
2	2	120	0.93039
3	4	140	0.96345
4	6	160	0.96185
5	8	180	0.99870
6	10	200	1.00000
7	12	220	1.00000
8	14	240	1.00000

Fig.2. $S(\gamma)$ for different reduction orders. Numbers of curve lines correspond to numbers of rows in the above table; the curve lines with numbers 6, 7, 8 coincide within the scale of the figure

It can be seen from the above data that almost one-hundred-percent solution convergence is observed in the reduction orders $m \ge 10$, $n \ge 200$. It should be also noted that the required number of Fourier's harmonics in field representations (53) outside of the fiber exceeds the number of similar harmonics in similar field representations (52) in internal cylinders by more than one order. This means that in the aforementioned method, as in the well-known electromagnetic field diffraction theory on the homogeneous cylinder (see. [22]), the main factor affecting the scope of computations is to provide a proper description of a rapidly oscillating field of the incident wave at the external boundary of the microstructured fiber by cylindrical harmonics. When exciting the microstructured fiber by the plane wave, the estimate $n > k_0 A$ [22] occurs. In the considered example we have $k_0 A \simeq 350$, and the

inequation $n \geq 200$ (see the above table) may be explained with the fact that the incident Gaussian-beam field distribution on the external boundary of the microstructured fiber proves to be more slanting if compared with the incident plane-wave field. In Fig. 3 and 4 the distributions $S(\gamma)$ are compared for cases when the radius A is close to A_c.
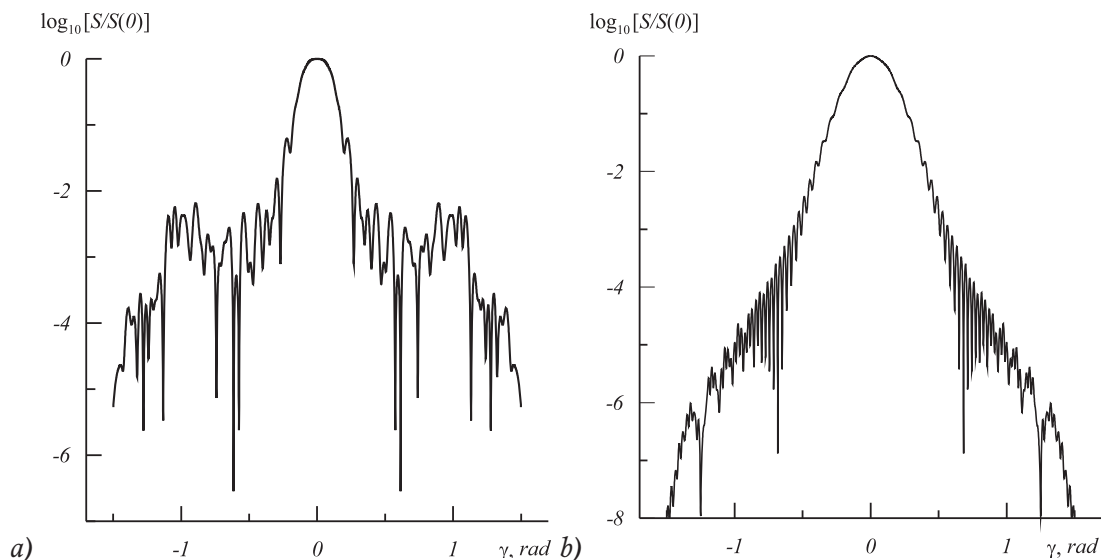
$\log_{10}[S/S(0)]$

a)

$\log_{10}[S/S(0)]$

b)

Fig.3. Distributions $S(\gamma)$ when exciting the microstructured fiber with $A = 19$ μm ($\Lambda = 1{,}672$ μm, $a = 0{,}089$ μm) (a) and $A = 18$ μm ($\Lambda = 1{,}584$ μm, $a = 0$ μm) (b) by TE polarized Gaussian beam
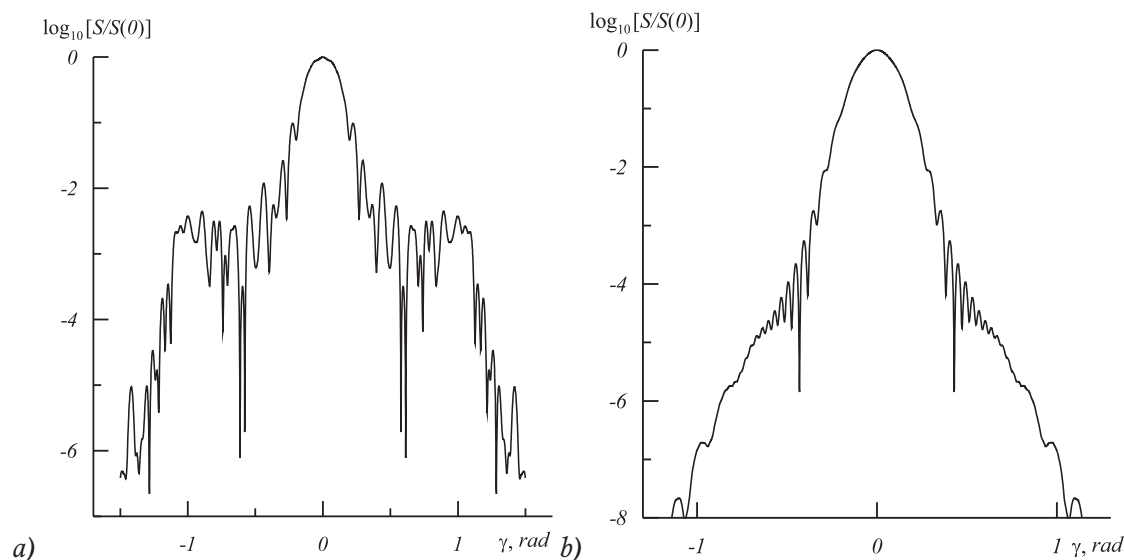
$\log_{10}[S/S(0)]$

a)

$\log_{10}[S/S(0)]$

b)

Fig.4. Distributions $S(\gamma)$ when exciting the microstructured fiber with $A = 19$ μm ($\Lambda = 1{,}672$ μm, $a = 0{,}089$ μm) (a) and $A = 18$ μm ($\Lambda = 1{,}584$ μm, $a = 0$ μm) (b) by TM polarized Gaussian beam

The curves in Fig. 3a and 4a correspond to the reduction orders $n \geq 10$, $m \geq 200$, and the curves in Fig. 3b and 4b – to $m \geq 200$ regardless of n. As seen from Fig. 3 and 4, the distributions $S(\gamma)$ being implemented when using the exciting TE and TM polarized Gaussian beams are similar ones. In both cases the blow-up of the air ports inside of the microstructured fiber results to high-quality resetting of distributions data. We can also conclude from Fig. 3 and 4 that if the air ports inside of the microstructured fiber have subwave lateral dimensions, then in order to provide their diffractive control the measurements of $S(\gamma)$ are required within the wide range of angles (in the considered examples we can perceive considerable influence of such air ports on the distribution $S(\gamma)$ when $|\gamma| > 0{,}25$ rad).

Conclusion

The angular distribution calculation of the far scattered-field intensity within the plane of incidence of the three-dimensional beam to the microstructured fiber in lateral light can be reduced to consideration of 2D diffraction problem. In order to solve the latter problem we have proposed the method based on the Green's theorem and the Graph's addition theorem. The method is simple enough in its numerical implementation and can be used for nondestructive diffraction control of microstructured fiber parameters. Its application has been illustrated with examples of construction of diffractive fields arising at excitation of the microstructured fibers by TE and TM polarized Gaussian beams.

References

1. Nguyen, H.C. New slant on photonic crystal fibers / H.C. Nguyen, P. Domachuk, B.J. Eggleton, M. J. Steel, M. Straub, M. Gu, M. Sumetsky // Opt. Express. – 2004. –Vol. 12(8). – P. 1530-1539.

2. Magi, E.C. Tapered photonic crystal fibers / E.C. Magi, P. Steinvurzel, B.J. Eggleton // Opt. Express. – 2004. –Vol. 12(5). – P. 776-784.

3. Magi, E.C. Transverse characterization of tapered photonic crystal fibers / E.C. Magi, P. Steinvurzel, B.J. Eggleton // J. Appl. Phys. – 2004. – Vol. 96(7). – P. 3976-3982.

4. Domachuk, P. Transverse characterization of high air-fill fraction tapered photonic crystal fiber / P. Domachuk, A. Chapman, E. Magi, M.J. Steel, H.C. Nguyen, B.J. Eggleton // Appl. Opt. – 2005. – Vol. 44(19). – P.3885-3892.

5. Minkovich, V.P. Holey fiber tapers with resonance transmission for high-resolution refractive index sensing / V.P. Minkovich, J.Villatoro, D. Monzon-Hernandez, A.B. Sotsky, L.I. Sotskaya // Opt. Express. – 2005. – Vol. 13(19). – P.7609-7714.

6. Minkovich, V.P. Modeling of holey fiber tapers with selective transmission for sensor applications / V.P. Minkovich, D. Monzon-Hernandez, J. Villatoro, A.B. Sotsky, L.I. Sotskaya // IEEE Journal of Lightwave Technology. – 2006. – Vol. 24(11). – P.4319-4328.

7. Brown, P.J. Photonic crystal-based fibers / P.J. Brown, S.H. Foulger // National Textile Center Annual Report. – 2005. – Project M02-CL06. – P.1-10.

8. Gauvreau, B. Color-changing and color-tunable photonic bandgap fiber textiles // B. Gauvreau, P.J. Brown, N. Guo, K. Schicker, K. Stoeffler, F. Boismenu, A. Ajji, R. Wingfield, C. Dubois, M. Skorobogatiy // Opt. Express. – 2008. – Vol. 16(20). – P.15677-15693.

9. Nesterenko, D.V. Light scattering by the dielectric cylinder including 2-D grating of metallic nanowires / D.V. Nesterenko, V.V. Kotlar // Computer Optics. – 2008. – Vol. 32(1). – P. 23-28. (In Russian).

10. Olaofe, G.O. Scattering by an arbitrary configuration of parallel circular cylinders / G.O. Olaofe // J. Opt. Soc. Am. – 1970. – Vol. 60(9). – P. 1233-1236.

11. Felback, D. Scattering by a random set of parallel cylinders / D. Felbacq, G. Tayeb, D. Maystre. // J. Opt. Soc. Am. – 1994. – Vol. 11(9). – P. 2526-2538.

12. Lee, S.C. Optical extinction by closely spaced parallel cylinders inside a finite dielectric slab / S.C. Lee, S. Chun // J. Opt. Soc. Am A. – 2006. – Vol. 23(9). – P. 2219-2232.

13. Frezza, F. Scattering by dielectric circular cylinders in a dielectric slab / F. Frezza, L. Pajewski, C. Ponti, G. Schettini // J. Opt. Soc. Am A. – 2010. Vol. 27(4). – P. 687-695.

14. Pawliuk, P. Scattering from cylinders using the two-dimensional vector plane wave spectrum / P. Pawliuk, M. Yedlin // J. Opt. Soc. Am. A. – 2011. – Vol. 28(6). – P. 1177-1184.

15. Yokota, M. Two-dimensional scattering of a plane wave from a periodic array of dielectric cylinders with arbitrary shape / M. Yokota, M. Sesay // J. Opt. Soc. Am. A. – 2008. – Vol. 25(7). – P. 1691-1696.

16. She, S. Improved Dirichlet-to-Neumann map method for scattering by circular cylinders on a lattice / S. She, Y. Lu // J. Opt. Soc. Am. A. – 2012. – Vol. 29(9). – P. 1999-2004.

17. Lee, S. Scattering by a radially stratified infinite cylinder buried in an absorbing half-space / S.C. Lee // J. Opt. Soc. Am A. – 2013. – Vol. 30(4). – P. 565-572.

18. Boyer, P. Differential theory for anisotropic cylindrical objects with an arbitrary cross section / P. Boyer // J. Opt. Soc. Am. A. – 2013. Vol. 30(4). – P. 596-603.

19. Sotsky, A.B. Theory of optical waveguide elements / A.B. Sotsky. – Mogilev: MSU Publisher. – 2011. – P. 456. (In Russian).

20. Marcuse, D. Light transmission optics / D. Marcuse. – Moscow: Mir Publisher. – 1972. – P. 576. (In Russian).

21. Abramovitz, M. Handbook of Mathematical Functions / M. Abramovitz, I. Stigan. – Moscow: Nauka. – 1979. – P. 830. (In Russian).

22. Ivanov, E.A. Diffraction of electromagnetic waves on two bodies / E.A. Ivanov. – Minsk: Nauka i technika. – 1968. – P. 584. (In Russian).

COMPUTER OPTICS